Connection between corner vortices and shear layer instability in flow past an ellipse

Z. Jane Wang
Courant Institute of Mathematical Sciences, New York University, New York, New York 10012

J. G. Liu
Institute for Physical Science and Technology and Department of Mathematics, University of Maryland, College Park, Maryland 20742

S. Childress
Courant Institute of Mathematical Sciences, New York University, New York, New York 10012

(Received 9 March 1999; accepted 2 June 1999)

We investigate, by numerical simulation, the shear layer instability associated with the outer layer of a spiral vortex formed behind an impulsively started thin ellipse. The unstable free shear layer undergoes a secondary instability. We connect this instability with the dynamics of corner vortices adjacent to the tip of the ellipse by observing that the typical turnover time of the corner vortex matches the period of the unstable mode in the shear layer. We suggest that the corner vortex acts as a signal generator, and produces periodic perturbation which triggers the instability. © *1999 American Institute of Physics.* [S1070-6631(99)04109-4]

Introduction. Vortex roll-up behind a sharp-edged body is a familiar phenomenon. In laboratory experiments, one finds that at high Reynolds numbers secondary vortices form along the outer layer of the primary vortex. A classical example of these beautiful secondary vortices can be found in the work of Pierce.[1]

However in those classical studies the origin of these secondary vortices was not clear. In an early work, Pullin and Perry[2] argued that the secondary vortices were the consequence of a shear layer instability, which could be triggered by oscillations in the experimental device. Using linear stability results for an exponentially stretching vortex sheet in an inviscid fluid and numerical studies of a self-similar vortex sheet,[3,4] they further predicted that the primary vortex should be stable in a viscous flow.

Recently, Koumotzakos and Shiels[5] simulated accelerating flows behind a plate using a vortex method, and they observed secondary structures similar to those seen in Pierce's experiment. These authors argued that the instability is intrinsic to accelerating flows.

There is also the possible contamination by numerical noise. For example, Krasny[6] has shown that both the round-off error and insufficient spatial resolution can introduce extraneous vortices, as have Brown and Minion.[7]

In this work, we reexamine, by direct numerical simulation, the shear layer instability which produces the secondary vortices. We consider a special case of impulsively started uniform flow normal to a thin ellipse, as opposed to accelerating flows studied by previous authors.[5] Secondary vortices are observed at sufficiently high Reynolds numbers, with $\mathrm{Re}=10\,000$ in our case. The periodicity associated with the secondary vortices is found to be independent of the numerical resolution. More interestingly, we also find a connection between the instability and the dynamics of small corner vortices,[2] which are adjacent to the tips of the ellipse and are induced by the primary vortices.

Flow setup and computational methods. We consider an impulsively started uniform flow normal to a thin ellipse of thickness ratio $h=1/8$. The Reynolds number based on the major axis L and flow velocity at infinity U_0 is $\mathrm{Re}=U_0L/\nu$, where ν is the kinematic viscosity. In our computation, $L=2$, $U_0=1$, and $\mathrm{Re}=10\,000$.

To simulate flow past an ellipse, we solved the Navier–Stokes equation in elliptic coordinates, (μ,θ). Elliptic coordinates can be mapped onto Cartesian coordinates via a conformal transformation, $x+iy=\cosh(\mu+i\theta)$. Consequently, the Poisson equation appearing in the Navier–Stokes solver has constant coefficients in the coordinates of (μ,θ), and it can be solved efficiently via Fast Fourier transform. The two-dimensional Navier–Stokes equation for vorticity has the following form in (μ,θ);

$$\partial(S\omega)/\partial t+(\sqrt{S}\mathbf{u}\cdot\nabla)\omega=\nu\Delta\omega, \tag{1}$$

$$\nabla\cdot(\sqrt{S}\mathbf{u})=0, \tag{2}$$

where $\mathbf{u}$ is the velocity field, ω the vorticity field, and S the scaling factor $S(\mu,\theta)=\cosh^2\mu-\cos^2\theta$.

Our Navier–Stokes solver is based on an explicit fourth-order compact finite difference scheme, recently developed by Liu and Liu.[8] A detailed description of the method can be found in Ref. 8. At the far field boundary, we impose the standard outer flow boundary condition for vorticity and use the potential solution of flow past an ellipse for the stream function. The numerical convergence study of the method has been established in Ref. 9.

To resolve the flow, we keep at least 10 grid points along the radial direction in the boundary layer, and at least 30 points in the azimuthal direction around each tip, whose length scale is estimated by its radius of curvature. Because the elliptic coordinates stretch exponentially at the far field, we can afford a large computational domain. In our studies, we chose the outer radius to be ten times the semimajor axis, which is sufficiently far away from the region of vorticity

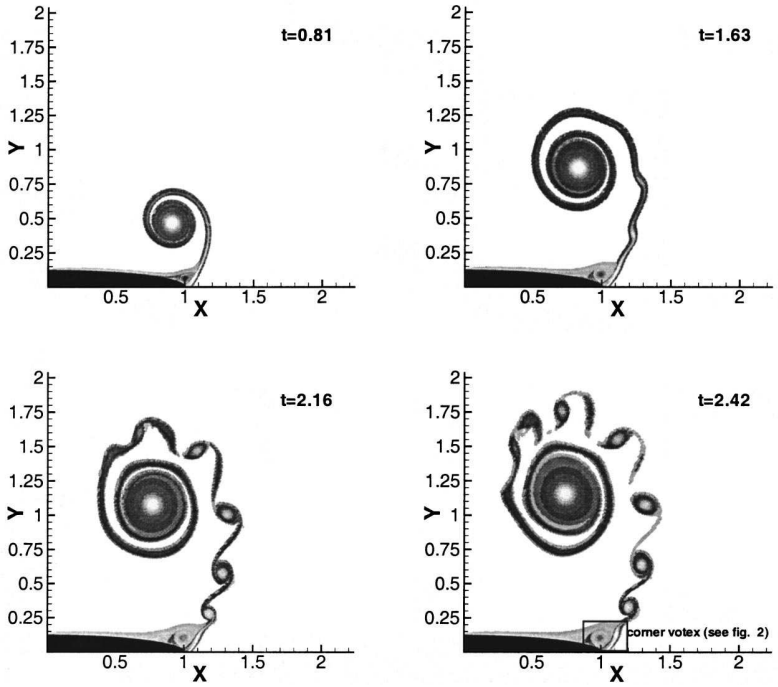

FIG. 1. Vortex growth as a function of time. Re $=10\,000$. Grid resolution 512×1024, with 1024 in the azimuthal direction. The gray scale corresponds to the strength of the vorticity. To save space, only the upper-right quarter of the region of the whole computation is shown. The detailed structure of the corner vortex inside the black box marked in plate (d) is shown in Fig. 2.

structure during the time of interest, $t\in(0,2.5)$. We also monitored the vorticity field near the far field to ensure that it was sufficiently small. For our computations its magnitude was on the order of the machine error. The computation was carried out using double precision for two resolutions: 512×1024 and 1024×2048. Finally, a single precision computation was performed to evaluate the effect of the round-off errors.

Results. In plates (a)–(d) of Fig. 1, we show the vorticity contour plot as time evolves up to $t=2.5$. The vortex development consists of two stages: (1) initial roll-up and growth of a primary vortex [plate (a)], and (2) formation and growth of periodic secondary vortices along the shear layer [plates (b)–(d)].

In addition to the primary vortex, we observe a hierarchy of small vortices at the corner bounded by the ellipse and the shear layer, as shown inside the marked box in plate (d). The hierarchy resembles the corner vortices in driven flows inside a box.[10] In our case, the small vortices are induced by the backflow of the primary vortex. The corner vortex system has been observed in previous experiments,[2] however its influence on the shear layer instability has not been studied.

In Fig. 2 we present the detailed structure of the secondary corner vortex. After an impulsive start, the corner vortex grows and reaches a quasisteady state. The elliptical asymmetry of this vortex can result in a periodic variation in the local vorticity field.

We plot the time series of the vorticity at various locations, marked by letters A–G in Fig. 2, inside the corner vortex. The results show periodic oscillations after an initial transient time. Fourier transforming the time series, we identify a period of oscillation, corresponding to $T\sim0.2$. This period turns out to match the temporal periodicity of the shear layer as we show below.

To estimate the temporal periodicity of the secondary vortex structure along the shear layer, we animated the computed time-dependent vorticity field. When playing back the animation, we placed a marker at a fixed point in the frame

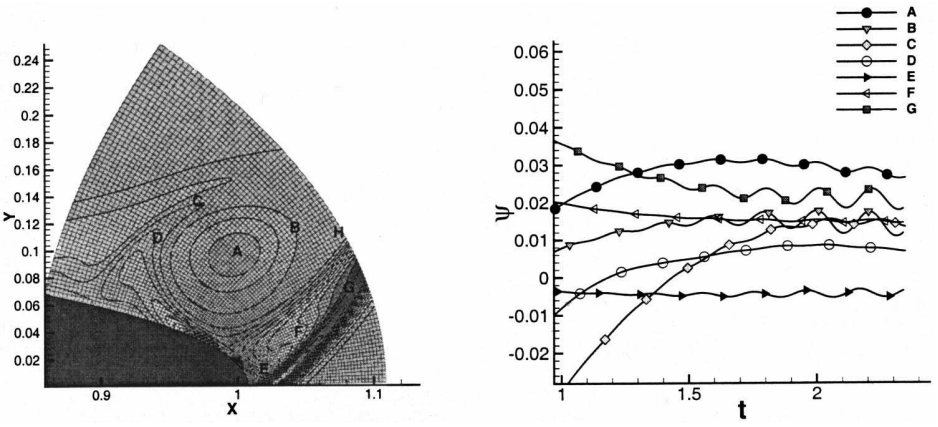

FIG. 2. The left-hand panel shows the zoom-in view of the vorticity contour plot near the tip of the ellipse. The computation mesh is also shown. The right-hand panel shows the time evolution of the stream function at various points near the tip. The same types of oscillations are seen in the vorticity field. However because the vorticity field is large inside the corner vortex, the superposed oscillations are not as obvious visually. We therefore chose to use the stream function Ψ for our diagnostics.

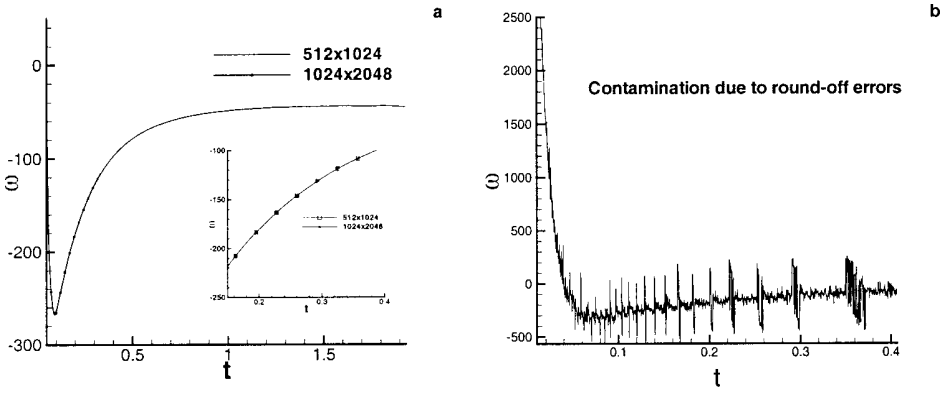

FIG. 3. (a) Comparison of the vorticity field with different resolutions: 512×1024, and 1024×2048. The inset shows the zoom-in view in the time window [0.15,0.4]. The vorticity is measured at the tip of the ellipse, which is most sensitive to the resolution. (b) Contamination due to round-off errors in single precision calculation. All other computation are done in double precision. The grid size is 512×1024. Note that these irregular noises are distinctly different from the well-defined periodic perturbation, see in Fig. 2. The contamination also occurs well before the onset of the secondary vortices in the resolved flows.

and counted the number of frames between two successive secondary vortices passing by the marker. This interval corresponds to the period. We repeated the same procedure for three consecutive vortex pairs, and the measurements were consistent. The estimated period is 0.21, approximately the same as the oscillation period of the corner vortex as shown previously.

To get an intuitive estimate of whether $T\sim0.2$ is a physical time scale, we note that in the corner vortex and the shear layer, $|\omega|\sim30-58$, which corresponds to a rotational rate $\Omega\equiv\omega/2\sim15-29$. This then gives a period $\tau=2\pi/\Omega\sim0.2-0.4$. Thus the observed period is consistent with the rotational rate of fluids in the corner vortex.

To confirm our results, we repeated our computation with twice the resolution, 1024×2048. In Fig. 3 we show vorticity at the tip of the ellipse as a function of time for these two different resolutions, and they agree remarkably well. We see no sign of grid oscillations. At the higher resolution, we ran up to time 0.35, limited by computing resources. The fact that the two curves agree in early times also shows that we have a good time resolution of an impulsively started flow as well as the spatial resolution. To investigate the effects of round-off errors, we computed the same flow using a single-precision computation. It is clear from the time series of the vorticity field that the large round-off errors in this case introduced irregular noises, seen in Fig. 3(b), which is distinctively different from the well-defined periodic variation in double-precision computations, as shown in Fig. 3(a). Furthermore, these errors can be detected directly with the time series of the vorticity field, well before the onset of the secondary vortex structure seen in the vorticity contour plot. This evidence make us believe that the secondary vortices seen in our computation are unlikely results of round-off errors. Finally, we checked the vorticity near the far field and find no background oscillation. We thus conclude that the observed instability is physical, and induced by activity at the corner vortex structure. We also remark that the instability is a high Reynolds number phenomenon. We do not observe it at $\mathrm{Re}=1000$, which is consistent with previous results.[5] Our results show that the instability is not unique to accelerating flows. In fact, these results suggest an alternative interpretation of the results in Ref. 5: The instantaneous Reynolds number increases with time in accelerating flows, and when it exceeds a critical Reynolds number, the secondary vortices appear.

Summary. We have computed flow past an ellipse at $\mathrm{Re}=10\,000$ to investigate the secondary vortex structure along the free shear layer of the primary vortex. We found that this secondary structure is connected with the dynamics of the corner vortex. Our study does not yet rule out the possibility that the oscillation in the corner vortex is simply responding to the shear layer instabilities. Future work is required to further distinguish these two possibilities.

ACKNOWLEDGMENTS

It is a pleasure to thank M. Shelley for many useful discussions, R. Krasny for communicating to us his recent work with M. Nitsche on oscillations of vortex pairs in inviscid flows, and H. Johnson for his help with improving the code. Z.J.W. acknowledges the support by NSF Grant No. DMS-9510356 and DOE Grant No. DE-FG02-88ER25053. The research of J.L. is supported by NSF Grant No. DMS-9805621, and of S.C. by NSF Grant No. DMS-9704546. We also thank NERSC for providing the supercomputer CPU time.

[1] D. Pierce, ''Photographic evidence of the formation and growth of vorticity behind plates accelerated from rest in still air,'' J. Fluid Mech. **11**, 460 (1961).
[2] D. I. Pullin and A. E. Perry, ''Some flow visualization experiments on the starting vortex'' J. Fluid Mech. **97**, 239 (1980).
[3] D. I. Pullin, ''The large-scale structure of unsteady self-similar rolled-up vortex sheets,'' J. Fluid Mech. **88**, 401 (1978).
[4] D. W. Moore and R. Griffith-Jones, ''The stability of an expanding vortex sheet,'' Mathematika **21**, 128 (1974); D. W. Moore, ''The stability of an evolving two-dimensional vortex sheet,'' *ibid.* **23**, 35 (1976).
[5] P. Koumoutsakos and D. Shiels, ''Simulations of the viscous flows normal to an impulsively started and uniformly accelerated flat plate,'' J. Fluid Mech. **328**, 177 (1996).
[6] R. Krasny, ''Desingularization of periodic vortex sheet roll-up,'' J. Comput. Phys. **65**, 292 (1986).
[7] D. Brown and M. Minion, ''Performance of under-resolved two-dimensional incompressible flow simulations,'' J. Comp. Physiol. **122**, 165 (1995).
[8] W. E and J.-G. Liu, ''Essentially compact schemes for unsteady viscous incompressible flows.'' J. Comp. Physiol. **126**, 122 (1996).
[9] H. Johnson and J.-G. Liu (unpublished).
[10] H. K. Moffatt, ''Viscous and resistive eddies near a sharp corner,'' J. Fluid Mech. **18**, 1 (1964).